SUPPLEMENTAL DATA

SUPPLEMENTAL EXPERIMENTAL PROCEDURES

Structure modeling- The structure model of NPC1L1-NTD protein was created by the ESyPred3D software with the crystal structure of human NPC1-NTD (PDB: 3GKI) as initial model. The cholesterol was superposed into the model from the structure of NPC1-NTD-cholesterol complex and check in Coot (1;2).

Coimmunoprecipitation- The procedure was performed as previously described (3). Briefly, the cells were treated as described in figure legends and then harvested and lysed in buffer A plus protease inhibitors. After centrifugation, the supernatants were incubated with anti-EGFP agarose and rotated for 2 hr at 4°C. Then the agarose was washed with buffer A for five times. Proteins bound to the agarose were eluted with buffer B, and neutralized with buffer C immediately. The eluted fractions were incubated in SDS-PAGE loading buffer at 37°C for 30 min. Immunoblot analysis was carried out as previously described (3).

SUPPLEMENTAL REFERENCES

1. Lambert, C., Leonard, N., De, B., X, and Depiereux, E. (2002) *Bioinformatics.* **18,** 1250-1256
2. Emsley, P. and Cowtan, K. (2004) *Acta Crystallogr. D. Biol. Crystallogr.* **60,** 2126-2132
3. Cao, J., Wang, J., Qi, W., Miao, H. H., Wang, J., Ge, L., Bose-Boyd, R. A., Tang, J. J., Li, B. L., and Song, B. L. (2007) *Cell Metab* **6,** 115-128
4. Kwon, H. J., bi-Mosleh, L., Wang, M. L., Deisenhofer, J., Goldstein, J. L., Brown, M. S., and Infante, R. E. (2009) *Cell* **137,** 1213-1224

SUPPLEMENTAL FIGURE LEGENDS

Fig. S1. The NPC1L1-NTD forms tetramer. Indicated concentrations of disuccinimidyl suberate (DSS) were incubated with NPC1L1-NTD solution for 30 min at 25°C, and then quenched by 30 mM Tris-HCl (pH7.4). The molecular weight shift of NPC1L1-NTD was determined by immunoblot.

Fig. S2. Comparison of NPC1L1-NTD and NPC1-NTD. (A) Sequence alignment of NPC1L1-NTD and NPC1-NTD. The identical and similar residues are shaded in black and yellow respectively. Blue asterisks denote residues that were predicted to line the cholesterol binding pocket of NPC1L1-NTD. Gray dots indicate the residues predicted in the binding pocket essential for the folding of NPC1L1. Red dots denote the residues predicted in the binding pocket dispensable for the folding of NPC1L1 but crucial for cholesterol binding. Green dot indicates the T128 residue predicted in the binding pocket not essential for the folding of NPC1L1 and cholesterol binding. (B) Ribbon diagram of the human NPC1-NTD structure with cholesterol solved by Kwon HJ et al (4). (C) The predicted structure of the human NPC1L1-NTD with cholesterol by homology modeling from the X-ray structure of human NPC1-NTD. (D) Diagram showing the magnified predicted binding pocket of human NPC1L1-NTD.

Residues predicted in the cholesterol binding pocket are indicated. Red denotes the residues crucial for cholesterol binding indicated in (Fig. 1C).

Fig. S3. The colocalization of Rab11a with indicated NPC1L1 variants. (A) The cells were co-transfected with plasmids encoding the indicated variants of NPC1L1-EGFP and Rab11a-RFP. 48 hr after transfection, the cells were fixed, and examined with confocal microscopy. Bar: 10 μm. (B) Quantification of the overlap co-efficient between the indicated NPC1L1 variants and Rab11a shown in (A).

Fig. S4. The colocalization of calnexin with indicated NPC1L1 variants. (A) The cells were transfected with plasmids encoding the indicated variants of NPC1L1-EGFP. 48 hr after transfection, the cells were fixed and immunofluorescence to label calnexin were performed. The cells were examined with confocal microscopy. Bar: 10 μm. (B) Quantification of overlap co-efficient between the indicated NPC1L1 variants and calnexin shown in (A).

Fig. S1

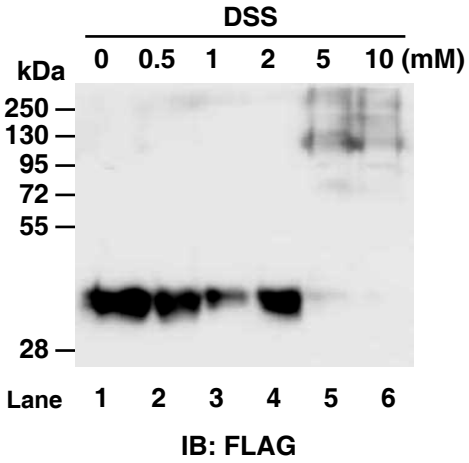

Fig. S2

A

```
human NPC1L1    1  MAEAGLRGWLLWALLLRLAQSEPYTTIHQPGYCAFYDECGKNPELSGSLMTLSNVSCLSN
human NPC1      1  MT-A--RGLALGLLLLLCPAQVFSQS-----CVWYGECG---IAYGD--KRYN--CEYS

human NPC1L1   61  TPARKITGDHLILLQKICPRLYTGPN-TQACCSAKQLVSLEASLSITKALLTRCPACSDN
human NPC1     46  GPPKPLPKDGYDLVQELCPGFFFG-N-VSLCCDVRQLQTLKDNLQLPLQFLSRCPSCFYN

human NPC1L1  120  FVNLHCHNTCSPNQSLFINVTR----VAQLGAGQLPAVVAYEAFYQHSFAEQSYDSCSRV
human NPC1    104  LLNLFCELTCSPRQSQFLNVTATEDYVDPVTNQTKTNVKELQYYVGQSFANAMYNACRDV

human NPC1L1  176  RVPAAATLAVGTMCGVYGSALCNAQRWLNFQGDTGNGLAPLDITFHLLEPGQAVGSGIQP
human NPC1    164  EAPSSNDKALGLLCGKDADA-CNATNWIEYMFNKDNGQAPFTITPVFSDFP---VHGMEP

human NPC1L1  236  LNEGVARCNESQGDDVATCSCQDCAASCPAIARPQALDSTFYLGQ  280
human NPC1    220  MNNATKGCDESVDEVTAPCSCQDCSIVCGPKPQPPPPAPWTILG  264
```

B NPC1

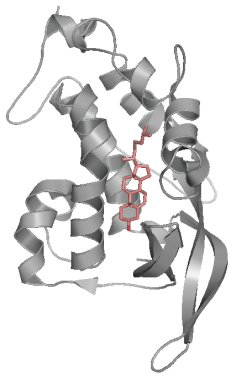

C NPC1L1

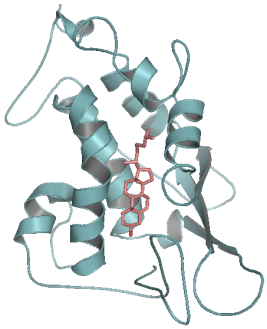

D NPC1L1

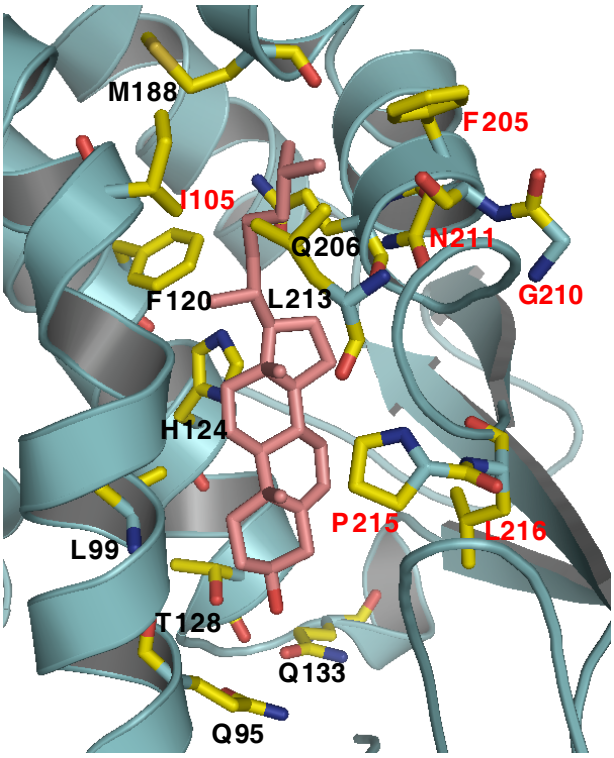

Fig. S3

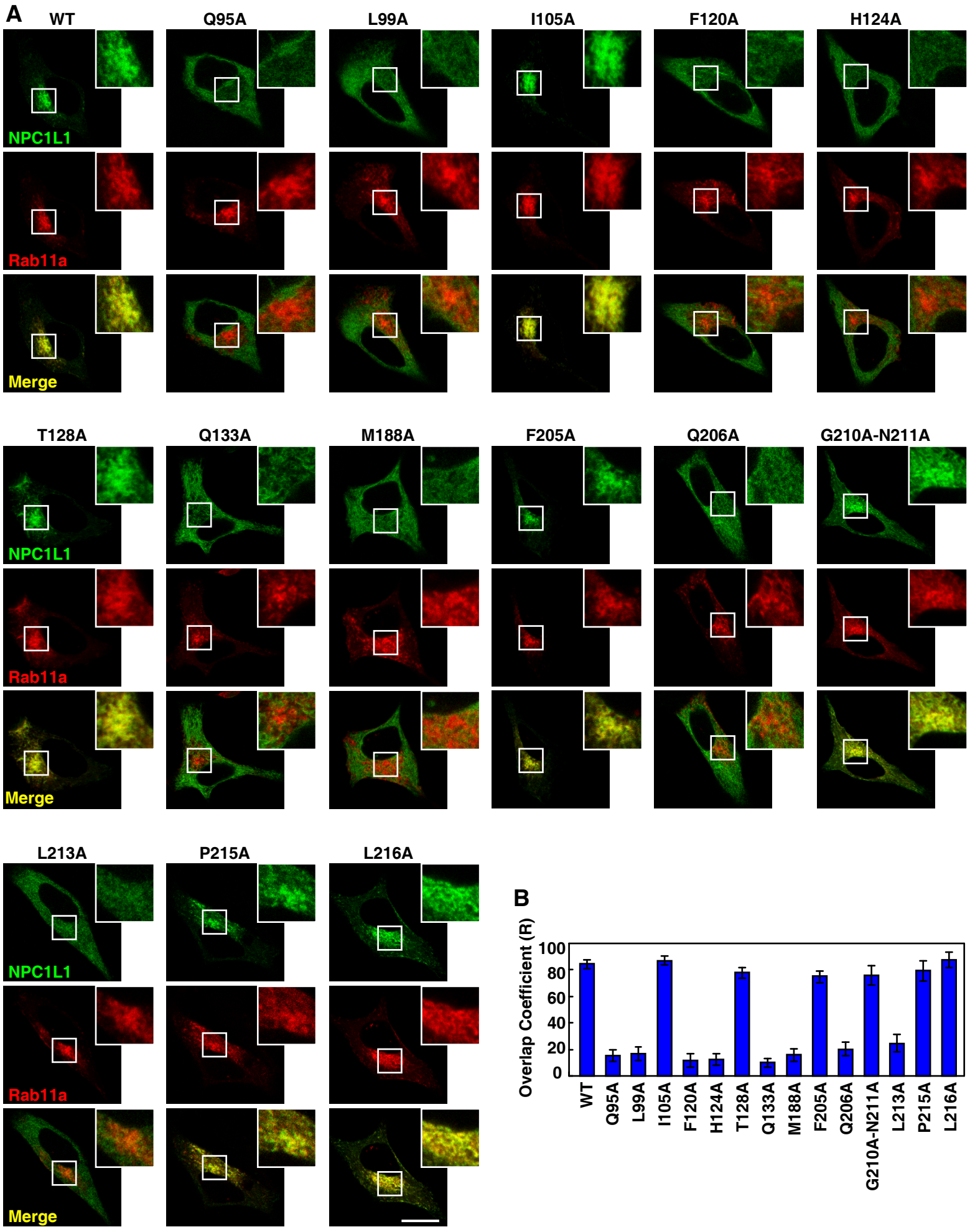
A
WT
Q95A
L99A
I105A
F120A
H124A
NPC1L1
Rab11a
Merge
T128A
Q133A
M188A
F205A
Q206A
G210A-N211A
NPC1L1
Rab11a
Merge
L213A
P215A
L216A
NPC1L1
Rab11a
Merge
B
Overlap Coefficient (R)
100
80
60
40
20
0
WT
Q95A
L99A
I105A
F120A
H124A
T128A
Q133A
M188A
F205A
Q206A
G210A-N211A
L213A
P215A
L216A

Fig. S4

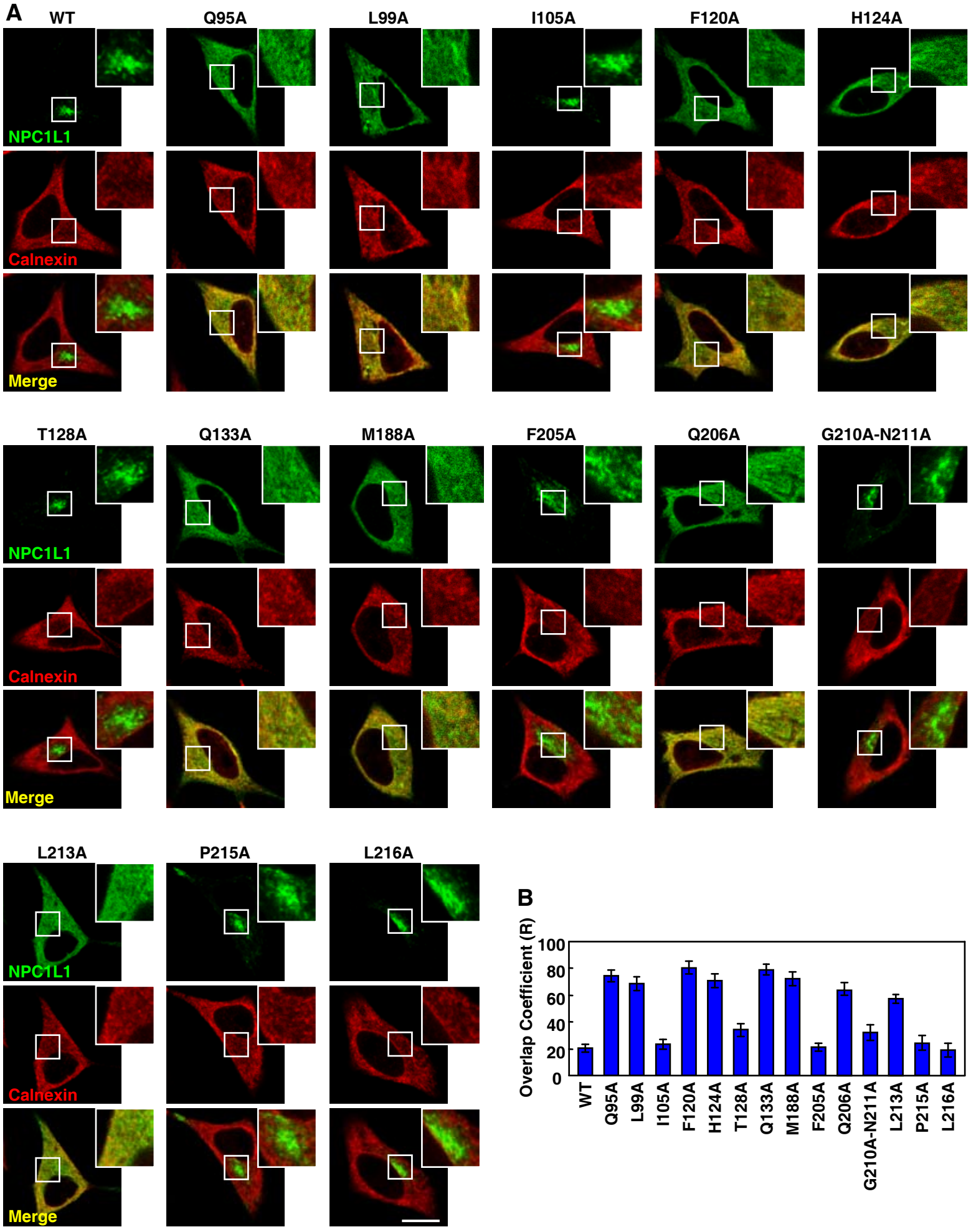
A
WT
Q95A
L99A
I105A
F120A
H124A
NPC1L1
Calnexin
Merge
T128A
Q133A
M188A
F205A
Q206A
G210A-N211A
NPC1L1
Calnexin
Merge
L213A
P215A
L216A
NPC1L1
Calnexin
Merge
B
Overlap Coefficient (R)
100
80
60
40
20
0
WT
Q95A
L99A
I105A
F120A
H124A
T128A
Q133A
M188A
F205A
Q206A
G210A-N211A
L213A
P215A
L216A